Underfill Flow in Flip-Chip Encapsulation Process: A Review

Fei Chong Ng
School of Mechanical Engineering,
Universiti Sains Malaysia,
Engineering Campus,
Nibong Tebal, Penang 14300, Malaysia

Mohamad Aizat Abas[1]
School of Mechanical Engineering,
Universiti Sains Malaysia,
Engineering Campus,
Nibong Tebal, Penang 14300, Malaysia
e-mail: aizatabas@usm.my

The scope of review of this paper focused on the precuring underfilling flow stage of encapsulation process. A total of 80 related works has been reviewed and being classified into process type, method employed, and objective attained. Statistically showed that the conventional capillary is the most studied underfill process, while the numerical simulation was mainly adopted. Generally, the analyses on the flow dynamic and distribution of underfill fluids in the bump array aimed for the filling time determination as well as the predictions of void occurrence. Parametric design optimization was subsequently conducted to resolve the productivity issue of long filling time and reliability issue of void occurrence. The bump pitch was found to the most investigated parameter, consistent to the miniaturization demand. To enrich the design versatility and flow visualization aspects, experimental test vehicle was innovated using imitated chip and replacement fluid, or even being scaled-up. Nonetheless, the analytical filling time models became more accurate and sophiscasted over the years, despite still being scarce in number. With the technological advancement on analysis tools and further development of analytic skills, it was believed that the future researches on underfill flow will become more comprehensive, thereby leading to the production of better packages in terms of manufacturing feasibility, performances, and reliability. Finally, few potential future works were recommended, for instance, microscopic analysis on the bump–fluid interaction, consideration of filler particles, and incorporation of artificial intelligence. [DOI: 10.1115/1.4050697]

Keywords: electronic packaging, flip-chip, package's reliability, underfill encapsulation, void occurrent

1 Introduction

Recent rapid advancement of micro-electronic industries demands faster and cheaper productions of miniature electronics devices with higher performance and reliability. Consequently, the flip-chip technology has seen various applications in micro-electronic packages and devices. In flip-chip packaging, the active side of the silicon die was faced downward and connected to the substrate via conducting bumps [1]. Flip-chip package undoubtedly is more advantageous than the conventional wire bond package in all aspects of input/output density, electrical performance, size, production cost, and thermal performance [2].

However, the major challenge posed by the flip-chip packaging is the thermal–mechanical stresses build-up due to the mismatch in the coefficient of thermal expansion (CTE) between the solder bump, silicon chip, and organic substrate. As the usage of electronic device persists, the interconnectors of chip package are subjected to thermal cycling and ultimately would result in fatigue or electrical failure. The CTE mismatch issue can be addressed by the underfill encapsulation process [2–4]. The narrow gap between the chip and substrate was filled with the underfill fluid which is the homogenous mixture of epoxy resin with fused silica fillers that will redistribute the thermal–mechanical stress away from the interconnectors [5]. Upon being cured, the underfill fluid that filled the gap between the bump array will chemically harden to form a protective layer that encapsulates the bumps. Despite the current described underfill process is conducted at the first level packaging of flip-chip, it is may be optionally carried out at the second level packaging between the IC package and printed circuit board, such as ball grid array (BGA).

Given the importances and viability of underfill process in addressing the shortcomings of flip-chip packages, it is still currently seen extensive applications in micro-electronic devices. Meanwhile, the underfill process still remains an active relevant research subject. Despite handful amount underfill researches being conducted to optimize and improve the process's productivity and later package's reliability, the comprehensive literature reviews on underfill works are still limited. There are only four review works related to the underfill encapsulation process being reported to date [2,3,6,7], as listed in Table 1. However, these reviews rather focused on a niche and narrow scopes. Moreover, as the latest review work being conducted back in 2014, the recent trends and advances of subsequent underfill researches were not discussed.

Therefore, an up-to-date review that encompassed on the latest researches is essential to provide insights on the recent advancement of underfill process and flip-chip technologies. Furthermore, the objectives of design optimization and enhancement works on underfill process have not been presented in detail.

This paper provided a comprehensive review on the past studies of underfilling flow in the encapsulation process, particularly on the visualization and modeling of underfill flow, together with the optimization works on the underfilling flow stage for the enhancement of the productivity of overall underfill process and later package's reliability. The past underfill studies were discussed based on the classifications of the type of underfill process investigated, the research methodology adopted, the underfill parameters optimized, and the research objective achieved.

2 Types of Underfill Encapsulation Process

There are three variants of underfill process on the first level packaging of flip-chip: capillary, no-flow, and molded [3], with their respective process flow schematics being illustrated in Fig. 1. All variants of underfill process comprised of two sequences, which is the initial underfilling flow and the subsequent post-underfill process of curing. Table 2 compared these three underfill

[1]Corresponding author.

Contributed by the Electronic and Photonic Packaging Division of ASME for publication in the Journal of Electronic Packaging. Manuscript received January 16, 2021; final manuscript received March 22, 2021; published online August 6, 2021. Assoc. Editor: Jin Yang.

Table 1 Overview of the past review works conducted on the scope of underfill encapsulation process

Year	Researchers	Review scopes	Highlights/concluding remarks	Reference
2004	Zhang and Wong	• Types of flip-chip underfill process	• New variations of underfill process were invented to address the shortcomings of conventional underfill process, for instance, no-fill, mold, and wafer level. • The process outline, material development, and reliability issues on each underfill process were detailed.	[3]
2007	Wan et al.	• Analytical and numerical modeling of underfill flow in the flip-chip encapsulation process	• The analytical filling time model developed by Wan et al. can predict the flow of non-Newtonian fluid. • For numerical simulation of underfill flow, Hele-Shaw approximation yields less accurate flow front prediction than the two-dimensional Navier–Stokes equations.	[2]
2012	Kim and Sung	• Analytical modeling of underfill flow • Visualization of underfill flow	• Three analytical filling time models were discussed and compared in terms of formulations and accuracies. • The underfill flow phenomenon of racing effect, voiding, and flow–bump interaction (i.e., contact line jump) was discussed.	[6]
2014	Khor et al.	• FSI studies on the mold underfill process	• FSI analysis is essential in the study of encapsulation process to determine the deformation of package during the dispensing of underfill fluid. • The challenges of FSI studies on package encapsulation modeling included complexity of package, simulation time, and computing limitation.	[7]

encapsulation processes, by outlining their process flow, as well the relative advantage and disadvantages.

The main difference among each underfill process is the process sequence of the initial underfilling flow stage, which later constitutes for the distinct underfill material compositions, package sizes, and dispensing setups. To speed up the capillary underfill process, no-flow underfill was introduced in which the underfill fluid was predistributed on the unmounted substrate before the chip being placed and affixed on it. Another variant of molded underfill was developed by injecting the underfill fluid into the chip assembly which is enclosed by a moldlike setup. Despite the no-fill and molded underfills resolved the productivity issue of slow underfill flow, the likelihood of occurrence of undesired voiding on the underfilled package greatly increases due to the uncontrolled distribution and rapid flow of underfill fluid, respectively. Additionally, the chemical reaction of fluxing agent in no-flow underfill during the thermal reflow induced void formation [8,9]. Moreover, both no-fill and molded underfills are less versatile as they required specific setups and limited for specific types of underfill fluid and design configuration of the chip packages. This is on top of additional manufacturing costs incurred as compared to conventional underfill fluid [2,3].

Alternatively, there are few modifications that were proposed on the conventional underfill process to accelerate the flow by applying external driving forces, for instance, forced/pressurized [10–12], vacuum-assisted [13,14], raised-die, substrate hole [3], rotational-assisted [15], and thermocapillary [16]. However, these creative iterations of underfill process were less popular as there is almost no application. This is because despite these improvised

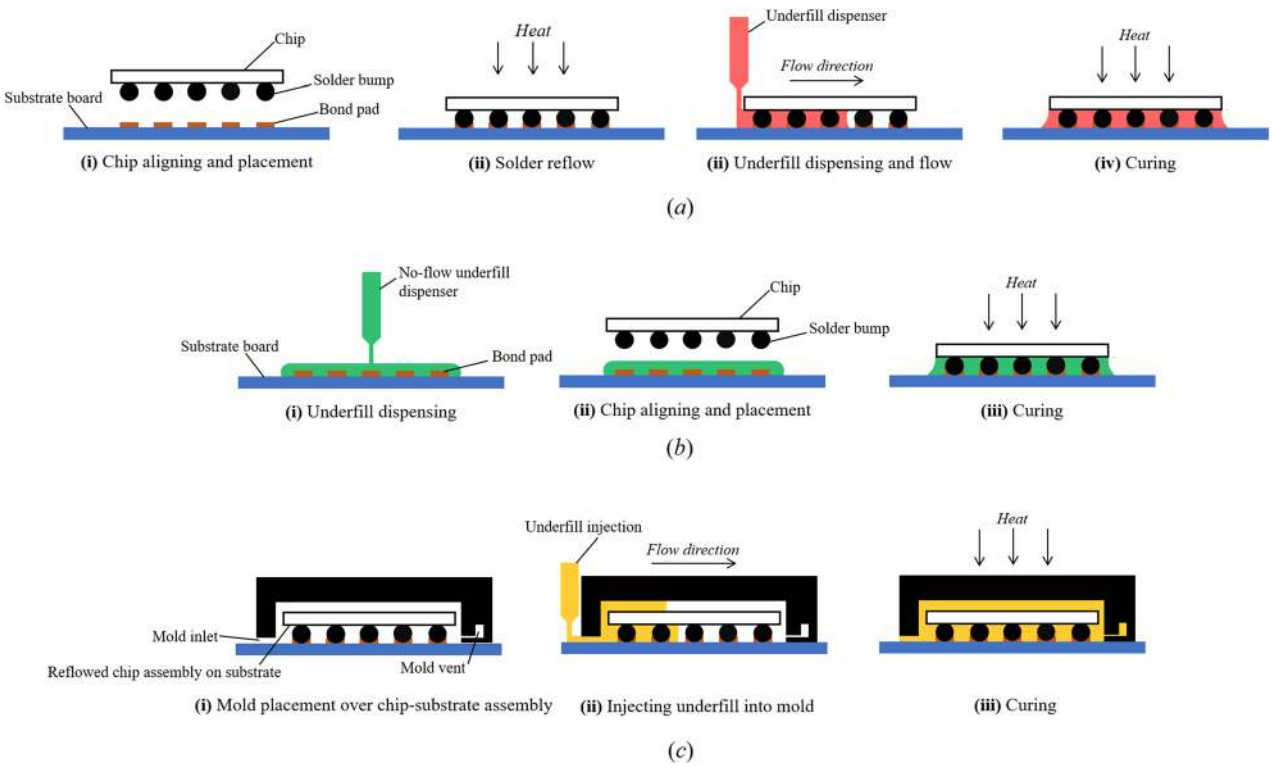

Fig. 1 Process flow schematics of various types of underfill encapsulations on chip device: (*a*) capillary underfill, (*b*) no-flow underfill, and (*c*) molded underfill encapsulation

Table 2 Overview on the various types of underfill encapsulation process

Types of underfill encapsulation process	Main outline of process flow	Advantage	Disadvantage
Capillary underfill	The underfill fluid was dispended along the one or more sides of package and been capillary driven onto the gap beneath chip and substrate. Finally, the underfilled package was sent to reflow oven for curing.	• Straightforward and the simplest process. • Ensure complete filling with lower occurrence chance of voiding and air entrapment. • Compatible for wide ranges of underfill fluids and package designs. • Can be reworkable.	• Slow capillary flow of underfill fluid, thus long process time.
No-flow underfill	No-flow underfill fluid with fluxing agent was predispended on the unmounted substrate board. Then, chip was aligned and placed vertically on the solder pads that redistribute the underfill fluid horizontally. Finally, the assembly was sent for reflow, to attach the bump on the solder pad as well as to cure the underfill fluid.	• Fast and simplified overall encapsulation process, with negligible filling time.	• High chance of voiding occurrent and incomplete filling due to the uncontrolled flow. • Excess underfill residuals between solder bump and bond pad may reduce connectivity, so the chip was forced onto the solder pad during the placement stage. • Require a specific type of underfill fluid premixed with the fluxing agent.
Mold underfill	A mold setup was placed over the chip–substrate assembly, and the underfill fluid was injected into the mold cavity. The underfilled assembly was cured first before removing the mold setup.	• Combined both over-molding and underfill in a single process, to reduce the process time. • Improves mechanical stability. • Molded underfill fluid (epoxy molded compounds) can contain higher silica filler contents than the conventional underfill fluid.	• Requires mold setup which incurs additional cost and setup time. • Possible occurrent of voiding and incomplete filling. • Low reworkability. • More underfill fluid is required to additionally over-mold the package.

underfill processes promoted the underfill flow, the manufacturing costs can greatly increase due to the need for process redesign together with the potential occurrence of voiding.

Upon comparing these variants of underfill process, the implementation of conventional capillary underfill is the simplest. Moreover, it is less prone to the defects of incomplete filling and void formation, but with the sole expense of long filling time. The conventional capillary underfill process still widely being adopted in industry because it does not require additional setups and specific variant of underfill fluid with additives. That is the advantages of capillary underfill which had outweighed its disadvantages.

3 Reviews of Past Works on Underfilling Flow in Flip-Chip Encapsulation

The scope of the current review work resides on the past researches that investigated the underfilling flow stage during the flip-chip encapsulation, for instance, in the stages illustrated in Figs. 1(*a*)(iii), 1(*b*)(ii), and 1(*c*)(ii). These underfill studies emphasized on the precuring stage when the underfill fluid was dispensed and being introduced into the gap between flip-chip package, for which it subsequently being filled, by means of flow or no-flow. All relevant works on the study of underfilling flow in encapsulation process were being classified accordingly based on the type of underfill process investigated, research method employed, and research goal achieved, while being sorted in the ascending order of the publication year. The comprehensive classifications on the past underfill flow studies were given in Appendices A–C, respectively, for the studies focused on the capillary, mold, and others underfill processes.

Figure 2 presents the number of researches that studied the underfilling flow in encapsulation process, based on the reviewed works listed in Table 3. Statistically, the researches on underfilling flow in encapsulation process show a gradual increasing trend, which implied that it still remains as an active and highly relevant research subject. The years 2010–2012 saw the most papers being reported in this short span of three years, which almost doubled the works over the last 14 years. It was followed by the most recent five years (2016–2020) which show a steady increasing trend. These data and growing trends also elicited that the importances of the underfill process in industrial and manufacturing practices, as well as the needs to enhance and optimize the underfill process as a joint improvement effort of package reliability. As such, it is expected more works will be conducted in the near future.

Table 3 further breakdowns the reviewed works listed in Table 2 according to the type of underfill process, research methodology, and research goal. Generally, the conventional capillary underfill is the most investigated underfill process, upon compared to the mold underfill and no-flow underfill. This is due to the capillary underfill process has the most industrial applications, apart from served as the fundamental study on underfill flow in bump array. On the contrary, no-flow underfill has the least amount of study as there is negligible underfilling flow stage in the no-flow underfill. In particular, almost all researches on no-flow underfill process

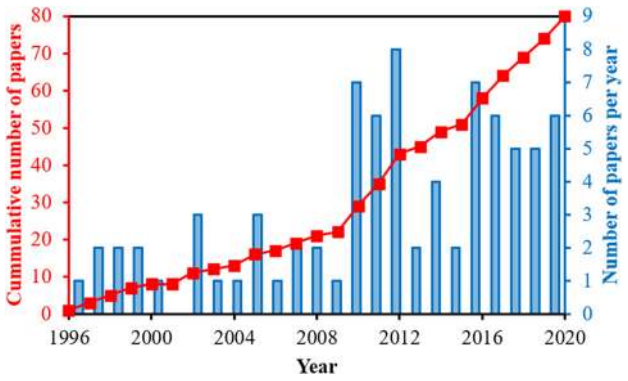

Fig. 2 Statistical trends on the study of underfilling flow in encapsulation process

Table 3 Statistics breakdown on the 80 reviewed underfilling flow works classified based on the type of underfill process, research methodology, and research goal

	Type of underfill process			
	Capillary	No-flow	Mold	Other
Number of papers	53	3	22	5
Percentage	66.25%	3.75%	27.50%	6.25%
	Research methodology			
	Experiment	Numerical simulation	Analytical formulation	
Number of papers	42	59	25	
Percentage	52.50%	73.75%	31.25%	
	Research goal			
	Design optimization	Package's reliability	Flow visualization and filling time determination	
Number of papers	40	30	72	
Percentage	50.00%	37.50%	90.00%	

emphasized on the post-curing stage, which mainly accessing the reliability issues of underfilled package (i.e., mechanical and voiding) rather than the productivity of underfill process. The mold underfill had seen heavy investigations during the peak years of 2010–2012, in which the fluid–structure interaction (FSI) phenomenon of mold encapsulated package was emphasized.

In terms of research methodology, the numerical simulation has seen most adoption, followed closely by experiment and finally being the analytical formulation. Despite the physical experiment is the most straightforward yet realistic approach, it lacks the customizability aspect for the design optimization study due to higher incurred costs and efforts. Furthermore, the flow visualization during the underfilling stage was hindered by the opaque nature package. Consequently, the numerical simulation rises as a prominent yet reliable alternative to model the underfill flow and subsequently for the optimization and process enhancement works. The third approach of analytical formulation which modeled the underfill flow based on the physics of fluid dynamics saw the least use in the literatures. This is mainly caused by the complexity of underfill flow in bump array to be modeled mathematically. Substantial assumptions were made to simplify the mathematical works but at the expenses of reduction in accuracy and yielded unrealistic depiction of the actual flow. Generally, the researchers tend to deploy the most appropriate methodological approach accordingly to align with their research objectives. Additionally, it is common for a study to consist of two or more methodologies, as most of the numerical simulated and analytical predicted findings were cross-validated experimentally.

Similarly, most of the underfill works reported tend to achieve more than one research goal. It was found that 90% of the underfilling flow studies aimed to visualize the underfill flow and to determine the filling time. Through the flow inspection, reliability issues such as racing effect and voiding could be observed, for subsequent root cause and mitigation analysis. Meanwhile, the filling time is the sole quantitative indicator to access the productivity of underfill process. In addition, half of the reviewed works involved in the design optimization of underfill process by manipulating the design parameters of package, process operating conditions, and material properties of the underfill fluid. There are handful literatures that attempted to address the reliability issues, for instance, voiding and package structural deformation. Nonetheless, all underfill researches shared a common objective of coherently improving both the productivity of underfill process and the package's reliability. Generally, these were achieved by resolving the two main issues arise in the underfill encapsulation process, i.e., prolonged filling time and void occurrence. It was believed that underfill flow stage not only incur longest manufacturing lead time but also responsible for the void formation.

4 Research Methodology

The methodological approaches used in the studies the underfill flow are physical experiment, numerical simulation, and analytical formulation, likewise in the other scientific fields. Figure 3 summarized the three main research methodologies found in the underfill flow studies. These approaches can be further classified accordingly their unique traits to ease the analysis on the trend of underfill researches. The experiment was categorized into the test vehicles adopted, either actual or imitated chip-underfill system. Furthermore, both numerical simulation and analytical derivation were decomposed according to their numerical discretization method and formulation approach, respectively.

4.1 Physical Experiment. Physical experiment is the most straightforward approach to investigate the flip-chip underfill process. Generally, the test vehicles used in the underfill experiment gradually shifting from actual chip and underfill fluid to imitated chip and replacement fluid, and finally to scaled-up imitation chip system, as depicted in Fig. 4. This transition from actual chip to imitated and finally scaled-up chip is aimed to enhance the flow visualization and to ease the manipulation of design parameters for optimization studies.

Actual chips and underfill fluids of industrial standard were used in the earlier underfill experiments, which gave the underfill flow profiles as shown in Fig. 4(*a*). Various types and designs of the packages were investigated, for instance, the IBM flower-array flip-chip [18], quadrilateral full array integrated circuit package [24,26], thin quad flat package (TQFP) [25], irregular middle empty flip-chip [17], and package-on-package device [31]. Moreover, all these experimental works have considered the non-Newtonian behavior of underfill fluids. The usages of industrial standard package and underfill fluid preserved most element of the industrial underfill process, thus ensuring the findings are accurate, practically consistent, and reproducible in the industry. These experimental findings from these literatures were served as a validating and benchmarking tool for the future works, particularly to verify the newly developed numerical and analytical models on flip-chip underfill process.

Apart from flow visualization and filling time measurement, experiments were also conducted for the purpose of material characterization [32,33], including the measurement of the material properties of underfill fluid such as viscosity [34,35], surface tension [18], and contact angle [36]. This is essential for the subsequent analysis of both numerical and analytical modeling of underfill flow, since the aforementioned parameters affected the flowability. As such, industrial underfill fluid was used to determine its rheological properties, which were fitted and represented

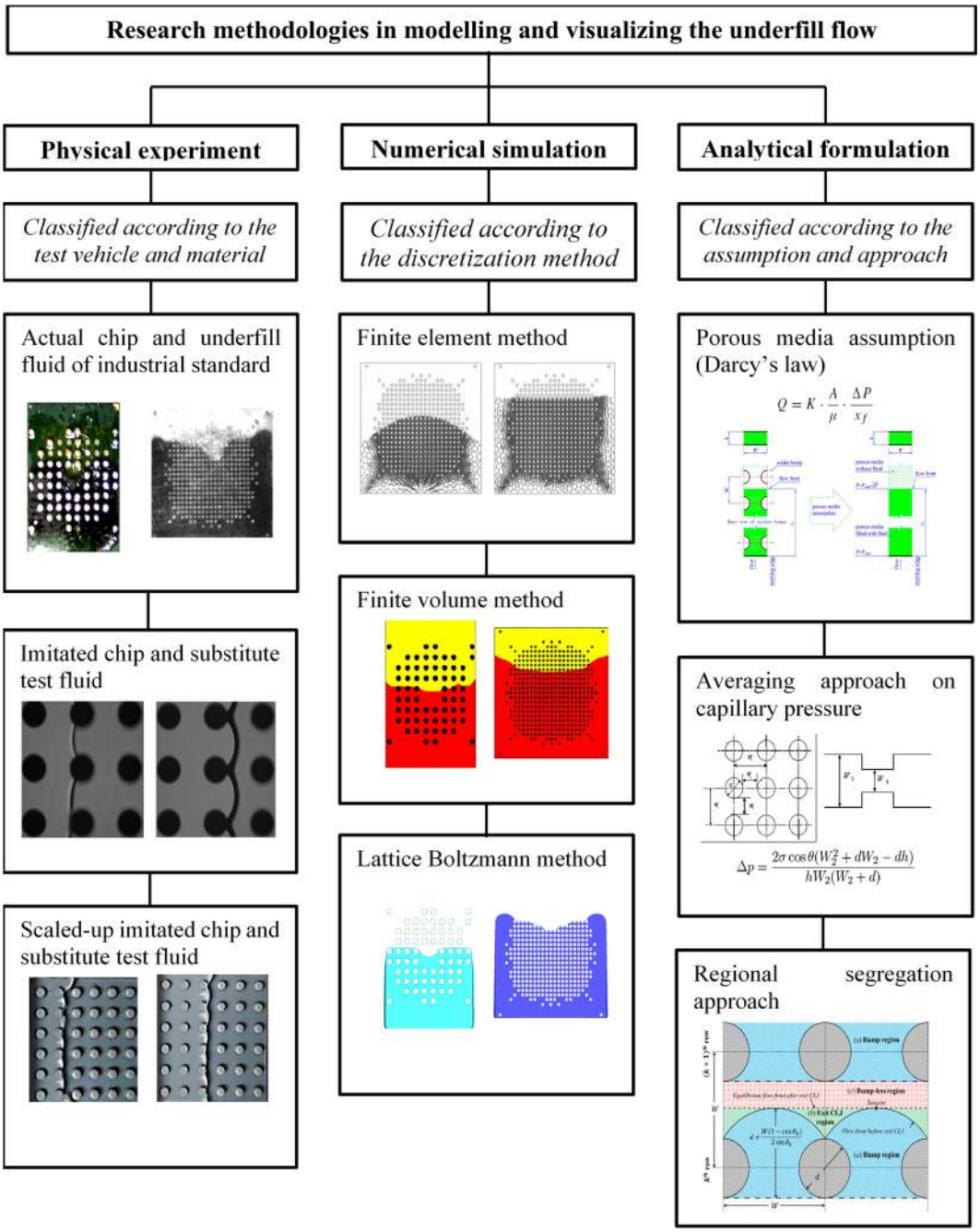

Fig. 3 Overview of underfill researches classified based on the research methodologies: physical experiment [17–20], numerical simulation [17,18], and analytical formulation [21–23]

by various models, for instance, power-law [24], Cox–Merx [18], Castro–Macosko [37,38], and Bird–Carreau [34].

The trend was shifting toward the use of substituting chip device and replacement fluid. Parallel plates being the simplest setup mimicking the capillary flow of underfill fluid in the narrow gap underneath the flip-chip package. It could be set up using two glass plates or a pair of quartz die and FR4 substrate [26]. Alternative iteration of slanted glass plate which gives a linear increasing gap height enables the variation study of gap height on the underfill flow [13]. The bump array in flip-chip can be reproduced by etching the silicon of a silicon on glass wafer into micropillar array [27]. This technique enables the production of flip-chip specimens with the desired dimensions and customizable designs to ease the experimental-based design optimization work. The sole requirement is that the surfaces of imitation chip must be smooth with low roughness, to mimic the actual chip and substrate surfaces.

At present, there is an experiment method of particle image velocimetry (PIV) being applied on the analysis of underfill flow dynamic, as depicted in Fig. 4(*b*). PIV is a nonintrusive flow visualization approach that generates the velocity contour of the investigated flow domain, which is hugely applied in the other fields of hydraulic and fluid dynamics [27,28,39]. The material requirements for the PIV experiment are transparent chip and translucent working fluid mixed with tracing particles. As such, the imitated chip made of transparent material (i.e., glass and Perspex) was adopted together with replacement fluid of glycerin [20,27]. PIV analysis on underfill flow is rewarding as it provided huge insights on the dynamic behaviors of underfill flow (i.e., meniscus evolution and contact line jump (CLJ)) as well as the flow streamlines

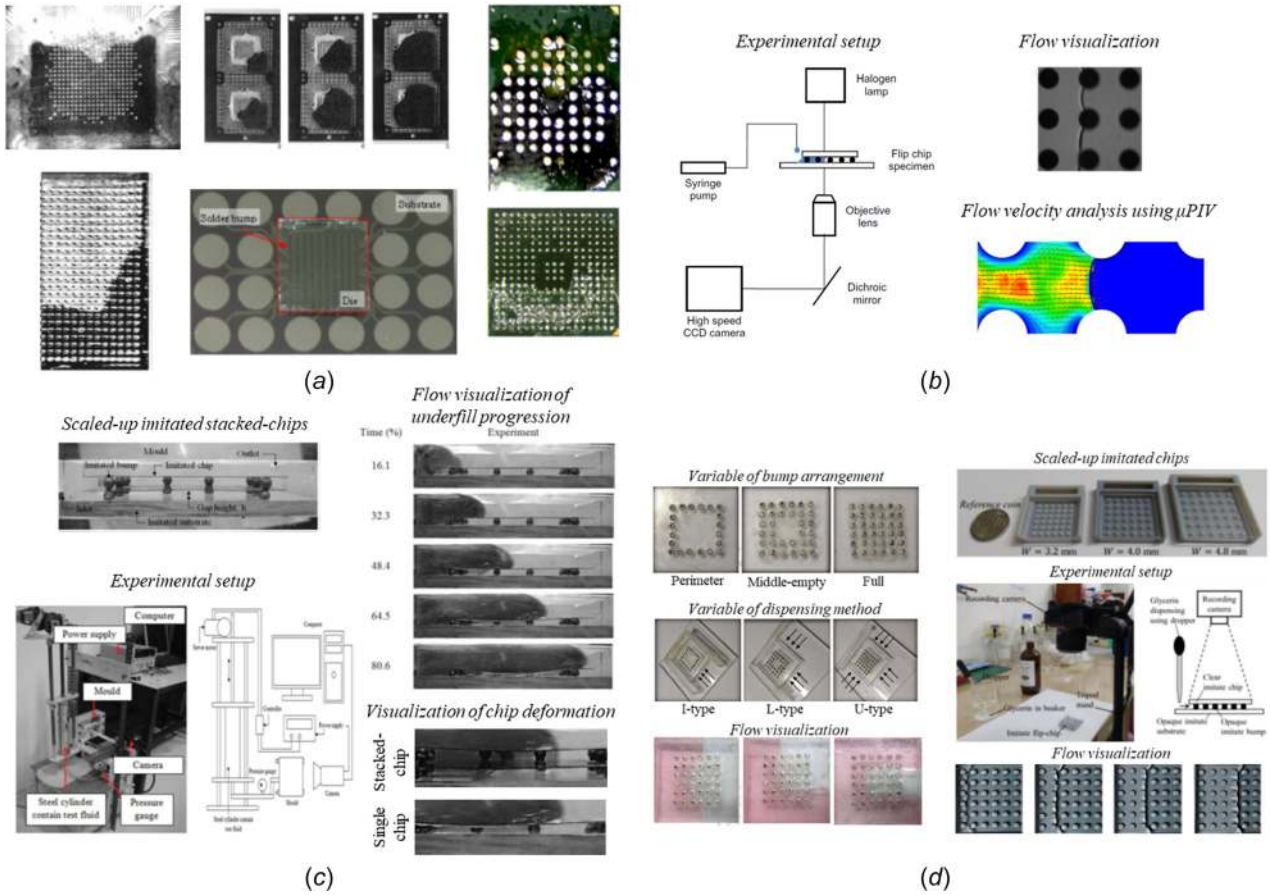

Fig. 4 Overview on the experimental approaches in studying the underfill flow of flip-chip encapsulation process: (*a*) actual experiment using chip and underfill fluid of industrial standard [17,18,24–26], (*b*) microparticle image velocimetry experiment using transparent imitated chips [27,28], (*c*) mold underfill experiment using scaled-up imitated chips [29], and (*d*) capillary underfill experiment using scaled-up imitated chips [20,30]

along the bump array. Nonetheless, the implementation of PIV on the study of underfill fluid is limited, as the flow velocity contour can be obtained numerically from simulation.

To future improve the visualization aspect, the proportional scaling method was applied on imitated chip package. Scaled-up imitated single and stacked packages were constructed for the experimental study of mold underfill process [29,40–44] as shown in Fig. 4(*c*), while scaled-up ball grid array model and flip-chip were used for the investigation of capillary underfill process [30,39,45–48] as depicted in Fig. 4(*d*). Similar scaled-up model was also applied in the study of pressurized underfill process. Such scaled-up models were also made of transparent material typically Perspex, to ensure swift construction. However, a major concern was raised regarding the scaled-up model is on the flow similarity and its ability to replicate the actual underfill flow. The scaling validity was analyzed and found that the scaling method is viable provided it is less than the scaling limit [20,39]. Qualitative comparable underfill flow fronts can be obtained, while the filling time of the flow in scaled model was also proportionally amplified by the same scaling factor [20].

The shifting from actual chip and underfill fluid to imitation chip and replacement fluid had been seen as a successful innovation to address technical issues of visualization and versatilities. Furthermore, the cross-validations using numerical simulation and analytical formulation addressed the concerns on reduced accuracy and the lack of practical depiction when using imitation chip and replacement fluid. Thus, it was inferred that the use of imitation and scaled-up chip models were well established and justified.

4.2 Numerical Simulation. Underfill flow in the flip-chip package was numerically simulated for flow visualization, filling time determination, as well as to obtain flow distributions of pressure, velocity, and temperature. Generally, in the underfill researches, numerical simulation was conducted together with corresponding experiment to cross-validate the findings. As shown in Fig. 3, the numerical works on underfill flow simulation can be classified based on the discretization scheme employed.

Prior to the emergence of finite volume method (FVM) based numerical simulation, earlier underfill simulations were based on finite element method (FEM). While FVM numerical approach is still seen as the most adopted method in underfill simulation to date, there is another mesh-less particle-based lattice Boltzmann method (LBM) numerical scheme being applied. Both FVM and FEM are largely similar in terms of formulation and discretization procedures, for except on the representation of differential equations (i.e., Eulerian against Langrangian coordinates systems) which were in integral form and basis form, respectively. Comparatively, FVM is easier to implement than FEM and LBM, due to the former Eulerian nature which fits well with fluid flow.

The earlier FEM-based underfill simulations mainly adopted the Hele-Shaw approximation [10,18,24,49–52]. However, this approximate is not viable, since the bump pitch is comparable to the gap size [2]. There is a commercially available simulation software, ANSYS, which ease the FEM modeling of fluid flow problem such as the underfill flow in encapsulation process [53].

Subsequently, the FVM-based ANSYS FLUENT software was introduced and applied for the modeling of underfill flow in various

types of underfill process including conventional capillary [20,30,39,47,54–57], mold [37,38,40,55,58,59], pressurized [11], and no-flow [60]. FVM simulation gives various data on the underfill flow, filling time, and flow's dynamic and thermal distributions. Moreover, ANSYS FLUENT software is advantageous as it could be extended for the further analyses, such as FSI [7,29,61], inclusion of the consideration of filler particles in underfill fluid [5], and incorporation of dynamic pressure boundary condition [62].

Fluid–structure interaction simulation approach was introduced in the studies of electronic packaging to investigate structural deformation of package due to the rapid injection of encapsulant during the mold underfill process. The packages studied included both single chip and stacked chips. FSI studied the simultaneous dependent and coupled interactions between both fluid flow and structural deformation [7,59,61]. Nonetheless, FSI is not useful for the study of conventional capillary process as the deformation on chip device is insignificant due to the slow underfill flow and negligible capillary force. Initially, FSI was setup using both FVM-based ANSYS FLUENT and FEM-based ABAQUS for the simulation of fluid and structural domains, respectively, subsequently were coupled by the mesh-based parallel code coupling interface [29,42,44,59,61]. With the advancement of simulation software, the FSI setup was simplified through the introduction of ANSYS System Coupling in which the whole FSI analysis could be done solely in FVM environment [16,47,63].

The flow simulation of underfill fluid with homogenous filler particles suspension was achieved by using discrete phase model in ANSYS FLUENT. Both the main constituents in underfill fluid of epoxy resin and silica fillers were separately considered to establish a two-way fluid–solid interaction with the aim to visualize the epoxy flow and filler particle distribution during the underfill flow stage [5]. On the contrary, other numerical studies on filler distributions were either based on the cured underfill package [64] or at the completion of underfilling [65]

In the recent years, particle-based LBM was used to simulate the underfill flow, which had seen various applications in conventional capillary underfill [12,17,45,46,48,66,67], mold underfill [68,69], and pressurized underfill [70]. While both LBM and FVM numerical findings are comparable in terms of flow visualization and filling time aspects, it is reported that LBM-based simulation can simulate the void formation during underfill flow for which FVM-based simulation is incapable to achieve [46]. Nonetheless, this shortcoming of FVM-based simulation was resolved by introducing micromesh unit-cell method for the underfill flow simulation to visualize the mechanism of void formation due to the fluid–bump interaction [57,71].

Apart from the well-known FEM and FVM as well as the emerging LBM, there are few underfill flow simulations that are based on novel numerical codes developed by respective researchers and are not bounded to any commercial software, for instance, finite different method (FDM) with pseudocompressibility approach and continuum surface force model [72], Petrov–Galerkin coupled with piecewise linear interface calculation-flow analysis network methods and level-set method [73]. Despite these new simulation approaches which gave reasonable prediction for underfill fluid, there is no future underfill work that is based on these methods, largely due to the lack of technical support for being noncommercial available simulation software.

4.3 Analytical Formulation. Generally, the analytical underfill studies are revolving around the determination of filling time, by deriving an equation relating filling time to filling distance and various design parameters. Nonetheless, these analytical-based studies are scarce in amount, with only eight distinct analytical filling time models being reported to date. This is caused by the complexity of mathematical formulation with limited understanding on flow dynamics, so the researchers tend to opt for straightforward experiment and simulation methodologies instead. Furthermore, the analytical models gradually become more sophiscasted and increasing accuracy, by considering more and realistic features of underfill flow in bump array.

Table 4 classified all eight analytical filling times available to date into the features of formulations. Generally, the main compositions of the formulation of analytical filling time models comprised of rheological model of underfill fluid, analysis approach, and governing equation, as summarized in Fig. 5. There are two main analysis approaches—namely, chip-level and bump-level—by considering the macroscopic and microscopic underfill flows, respectively. In chip-level analysis, the driving capillary pressure is averaged, and the whole bump array is collectively characterized into a single flow domain, for instance, as a porous media with known porosity and permeability. Meanwhile for the bump-level analysis, the dynamic of underfill flow was considered at every flow distance microscopically, in which the capillary pressure bump varies at different locations. In terms of governing equation, if the chip-level analysis adopted porous media assumption, Darcy's law will be governed; otherwise, the bump-level analysis would be based on the momentum equation. For the models considering the non-Newtonian rheological behavior of underfill fluid, only the power-law equation being was adopted owning to its mathematical simplicity.

About a century ago, Washburn equation was derived to relate the relationship between the filling time, t_f, and filling distance, x_f, for the capillary–viscous flow in horizontal gap between two parallel plates

$$t_f = \frac{3\mu x_f^2}{\sigma h \cos\theta} \tag{1}$$

where μ is the dynamic viscosity, σ is the surface tension, h is the gap height, and θ is the contact angle at the plate surface [18]. Nonetheless, Washburn equation did not incorporate the bump effect until the variable capillary pressure difference of meniscus due to varying gap and orientation between two adjacent bumps of pitch W was formulated as a function of bump angular displacement, ϕ

$$\Delta p(\phi) = \frac{2\sigma\cos\theta}{h} + \frac{2\sigma\cos(\theta+\phi)}{W - d\cos\phi} \tag{2}$$

This regards as the cornerstone of bump-level analysis for the capillary underfill flow [74].

Statistically, there are four models based on the chip-level analysis and two models based on the bump-level analysis. Among three chip-level analysis-based models which were established upon the porous media assumption with averaged capillary pressure and governed by Darcy's law as follows:

$$t_f = \frac{\mu\varepsilon}{2k\Delta\bar{p}} x_f^2 \tag{3}$$

with the porosity, ε, and the permeability, k, associated with the porous flow domain of the bump array. The main differences between these models are largely on the determination of averaged capillary pressure and permeability of the flow domain. The sole chip-level analysis-based model governed by the momentum equation and power-law rheological model averaged the capillary driving pressure by means of virtual force to yield the most elegant form of filling time model

$$t_f = \frac{2n+1}{n+1}\left[\frac{mhW(W+d)}{2\sigma\cos\theta\,(W^2+dW-dh)}\right]^{\frac{1}{n}}\left(\frac{2x_f}{h}\right)^{\frac{n+1}{n}} \tag{4}$$

where m and n denoted the flow consistency index and flow behavior index, respectively, for a non-Newtonian power-law fluid [22].

On the contrary, the bump-level analysis had been applied in two applications for the development of filling time model

Table 4 Classifications of analytical filling time models for the prediction of filling times of flip-chip underfill encapsulation process

Analytical filling time model	Washburn	Young	Young	Wan	Young	Yao	Luo	Ng
Year	1921	2003	2004	2005	2010	2014	2016	2019
Reference	[18]	[51]	[74]	[22]	[75]	[21,76]	[77]	[23]
Bump shape	Not considered	Cylinder	Cylinder	Square	Not considered	Cylinder	Square	Cylinder
Analysis type	Parallel plates	Chip-level	Bump-level	Chip-level	Parallel plates	Chip-level	Chip-level	Bump-level
Fluid viscosity	Newtonian	Newtonian	Newtonian	Non-Newtonian power-law	Non-Newtonian power-law	Newtonian	Newtonian	Non-Newtonian power-law
Temporal governing equation	Momentum	Darcy's law	Darcy's law	Momentum	Momentum	Darcy's law	Darcy's law	Momentum
Spatial governing equation	Not applicable	Geometrical shape of flow meniscus	Geometrical shape of flow meniscus	Not applicable	Not applicable	Geometrical definition of contact angle	Not applicable	Geometrical definition of contact angle
Capillary pressure	Constant	Averaged over one pitch	Variable	Averaged over one pitch	Constant	Averaged over one pitch	Averaged over one pitch	Variable
Contact line jump	Not applicable	At entrance only	At entrance only	Not considered	Not considered	Both entrance and exit	Not considered	Both entrance and exit

[23,74]. Generally, the bump-level analysis is coupled with the regional segregation approach, in which the filling times were computed separately at different locations based on the flow characteristics and the presence of bumps. As such the capillary pressure was not averaged but instead varies according to the filling location. Initially, the bump-level analysis considered the dynamics of underfill flows on both the region confined between two adjacent bumps and the region without bump confinement [74], until later the third region of exit CLJ being incorporated [23]. CLJ is the instantaneous change of meniscus shape when it approaches or leaving the bump surface [51,74]. Moreover, it was found that the CLJ effect when the underfill fluid exiting the bump array took substantially longer than when entering the bump array [27]. This justified the need of additionally considering the filling time during the flow of exit CLJ.

5 Design Optimization of Underfill Parameters

One of the main interests in underfill encapsulation researches is to optimize the parameters associated with the underfill encapsulation process to increase the productivity of manufacturing process and the reliability of micro-electronic package. Improvements of both aspects would reduce the manufacturing costs, while the device could last longer with better performances, in turns benefitting the end consumers. Figure 6 summarized the three main aspects of underfill associated parameters being optimized in the past researches, for instance, design parameters of chip package, material properties of underfill fluid, and operating conditions of underfill process. Subsequently, Tables 5 and 6 highlighted the variation effects of various underfill parameters on the filling time and void occurrence, respectively.

As the recent advancement of micro-electronic industry favors the miniaturization trend, smaller and more compact and high performing micro-electronic packages (e.g., chip and integrated circuits) were designed. Consequently, the package's size became smaller with higher number of input/output interconnection bumps, giving a higher bump density but smaller bump pitch. Smaller pitch size not only lengthen the filling time but also increase the likelihood of void occurrence. Studies suggested that the bump pitch should exceed its critical value, or else the filling time increases significantly. Additionally, the gap height is another important parameter to be considered, as small gap does not favor the underfill flow and substantially lengthen the filling time. From the qualitative aspect of package design of bump shape, bump with narrow neck yields faster underfill flow. There is another attempt to achieve high performing miniature package is by stacking multiple chips vertically upward, forming the package-on-package. However, stacking causes more void formation, and the void counts increase with the stacked layer and row. Despite the current trend of package miniaturization which can increase both the compactness and performance of device to comply with the current technological needs, the subsequent underfill encapsulation process would suffer from both productivity and reliability issues. Accordingly, optimization work is crucial to achieve an optimized package of high performance and reliability which at the same also manufacturing feasible and productive.

Generally, the underfill fluid of higher filler content is preferred and performed better in addressing the CTE mismatch issue of package. Nonetheless, the increases in filler loading also increased the viscosity and thus reduced the flowability, while also prone to another reliability issue of filler settling. Underfill fluid with higher filler loadings tends to exhibit as non-Newtonian fluid, in which the filling time increases with the power-law index. Ideally, the underfill fluid with low viscosity and high wettability (i.e., high surface tension and low contact angle) has good flowability, thereby giving shorter filling time. Nonetheless, the underfill fluid of high viscosity and low Bond number can lower the voiding occurrence.

The process operating conditions were manipulated to reduce the filling time and void occurrence. Generally, dispensing

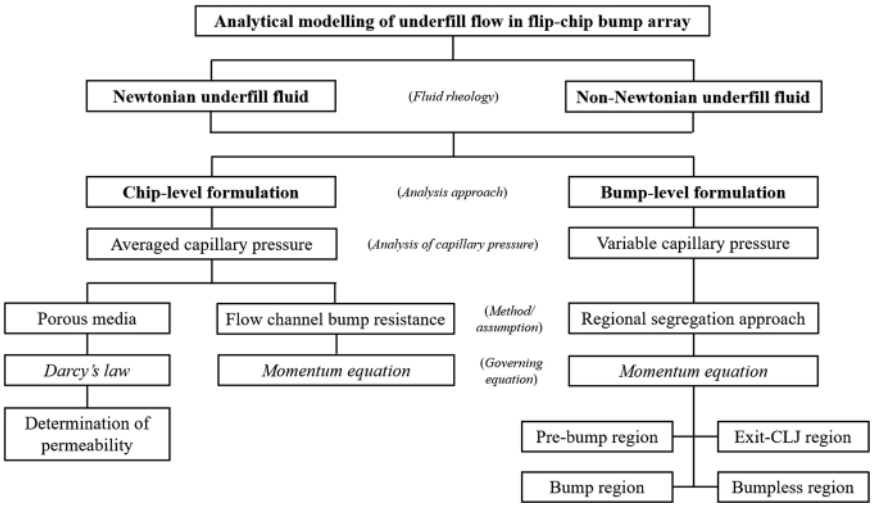

Fig. 5 Classifications on the formulations in the analytical modeling of underfill flow in flip-chip bump array for the development of filling time model

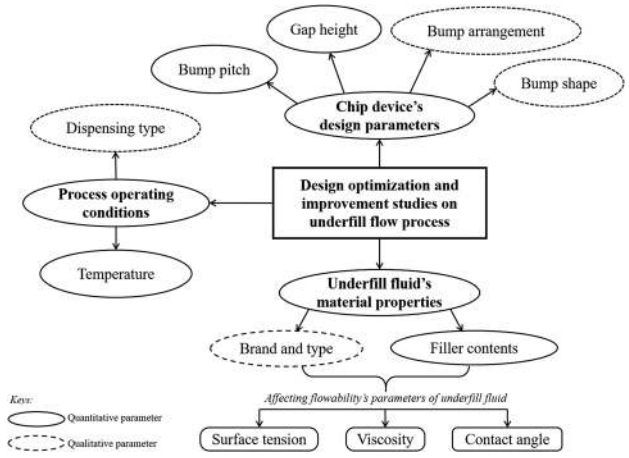

Fig. 6 Overview on the parametric design optimization studies on the underfill flow in flip-chip encapsulation process

method with more inlets could reduce the filling time in a larger extend. Nonetheless, the triple inlet dispensing (U-type) exposed to higher risks of void formation. As such, the double inlet dispensing (L-type) with lesser voidability was determined as the optimized dispensing method that is balanced from both aspects of filling time and voiding. Another operating parameter being studied is the dispensing and process temperature, in which the flowability of underfill fluid increases with the temperature.

6 Conclusions

Various researches were devoted to improving the productivity of underfill process and package's reliability. As the underfill dispensing and flowing stage took the substantial fraction of lead time in the whole underfill process, it became the prime focus in the optimization works. Moreover, the voids could be formed as early during the underfilling flow stage. Therefore, there are handful amount of works which analyzed and modeled the underfill flow in flip-chip package.

This paper reviewed the past works that focused on the underfilling flow stage in the flip-chip encapsulation process. As such, the studies on the curing stage and post-encapsulation analysis on the encapsulated package (e.g., cross-sectional inspection and structural strength testing) were not included. A total of 80 relevant works reported over the last 24 years were reviewed and classified based on the type of underfill process investigated, the research methodology employed, and the research objective attained. It was found that conventional capillary underfill is the most studied underfill process, followed by mold underfill and finally no-flow underfill. Furthermore, most researches adopted at least two methods, with the most common pair being simulation and experiment. Numerical simulation is the most applied method,

Table 5 Overview of parametric design optimization studies on the filling time of underfill process

Parameters	Findings on the trend of filling time
Bump pitch	• Smaller bump pitch yields longer filling time [23,27,49,50,78,79]. • The filling time increases significantly if the bump pitch is less than a critical value of pitch size [31,80]. • The trends of bump pitch depended on the critical contact angle. For contact angle lower than its critical value, the filling time increases with pitch; otherwise, the filling time increases with the decrease of pitch [31].
Gap height	• Smaller gap height resulted in slower underfill flow and longer filling time [13,47,55].
Bump arrangement	• Lower bump count on a package (resulted from bump arrangement) reduces the filling time, such that the perimeter bump array gives the lowest filling time, while the full bump array has the longest filling time [30,43,46,52,81].
Bump shape	• Bump with the characteristics of narrow neck, low sphericity, and high pad-to-neck ratio can give to shorter filling time [39].
Filler contents	• Higher filler contents increase the viscosity of underfill fluid, thus longer filling time [5,35].
Viscosity	• Viscosity is directly proportional to the filling time [18,36].
Surface tension	• Surface tension is inversely proportional to the filling time [30,45,81].
Power-law index	• For non-Newtonian underfill fluid, the filling time increases with the power-law index [82].
Contact angle	• Lower contact angle gives shorter filling time [37].
Dispensing type	• Multiple dispensing edge inlets shorten the filling time, such that triple inlet dispensing (U-type) gives shortest filling time [37].
Temperature	• Increase in temperature decreases the viscosity of underfill fluid, thus decreases the filling time [37]. • The implementation of thermal gradient across package layers can promote the underfill flow, compared to the isothermal setup [16].

Table 6 Overview of parametric design optimization studies on the voiding occurrence

Parameters	Findings on the trend of voiding
Bump pitch	• Smaller bump pitch causes more voids' formation [83].
Gap height	• The increases in gap height increases the void formation occurrent together with the size of void formed [48,84].
Bump arrangement	• Middle empty bump arrangement has the highest void occurrence but of smaller sizes, as compared to the full and perimeter arrangements [39,45–47].
Viscosity	• Voiding occurrence can be reduced by decreasing the surface energy of substrate or increasing the viscosity of the underfill fluid [35,45,46].
Dispensing type	• For no-flow underfill, dot dispensing pattern gave the least void formation as compared to the cross pattern [60]. • For capillary underfill, U-type dispensing yields higher void occurrence than both L-type and I-type dispensing [30,48,85]. • For mold underfill, the void occurrence decreases with the introduction of vacuum, while better vacuum quality gives smaller voids formed [14]. • For mold underfill, typical inlet gate gives less void occurrent compared to both diagonal and top center inlet gates [40,58].
Stacking of chips	• The stacking of chips caused more void formation [40]. • The occurrence of void formation was affected by the stacking layout [68]. • The number of void counts in stacked package increases with both the number of vertical stacked chips and the row of stacked chips [38].

but the analytical formulation has the least adoption. 90% of works focused on the flow visualization and filling time determination, while about half of them involved in the design optimization of underfill parameters.

The parametric design optimization studies generally focused on the reduction of both filling time and void occurrence, while the bump pitch is the most manipulated variable consistent to the recent miniaturization trend. The shortest filling time can be obtained from the combination of low viscosity, low contact angle, high surface tension, large gap height, and huge bump pitch. Nonetheless, low viscosity leads to higher void occurrence; thus, the viscosity needs to be optimized. Additionally, small pitch size, multiple inlets dispensing condition, and stacking of package are also prone to void formation.

As the past underfill studies were mainly emphasized on the macroscopic analyses (i.e., filling time, pressure, velocity, and temperature), it was recommended for the future underfill works would be based on the targeted analysis of microscopic aspects. The foremost being the interaction between underfill fluid and solder bump. As the solder bump array hindered the flow advancement, it would prolong the filling time and caused air entrapment in the bump vicinity. Through microscopic analysis of capillary flow along the bump array, the exact flow and voiding mechanisms with the corresponding flow distributions could be obtained. Additionally, the filler particles suspended in underfill fluid should be considered and investigated in the underfill flow studies as they are integral to the fluid's rheological behavior and ultimately affecting the outcomes of underfill process. Proper optimization on the size and type of filler particle as well as the filler contents is essential to improve the flowability of underfill fluid and to reduce the occurrence of filler settling defect. Furthermore, the incorporation of resilience and self-healing concepts on the industrial underfill system is worth for future exploration to attain ecosystem sustainability [86]. Finally, to align with the recent trend of industrial implementation of artificial intelligence, it was suggested that the future underfill flow studies to employ the machine learning approach. This would greatly benefit the design optimization of flip-chip package and underfill fluid material, as a joint effort to improve the process productivity.

Funding Data

- Fundamental Research Grant Scheme (FRGS) (Grant No. 203/PMEKANIK/6071428).
- Research University (RU) (Grant No. 8014071).

Appendix A: Summary of Past Research Works on the Study of Underfilling Flow Stage in the Conventional Capillary Encapsulation Process

Year	Research method	Research goal	Highlight on main finding	Reference
1996	• Analytical (Washburn equation) • Experiment (parallel plate)	• Filling time measurement/ predi ction • Design optimization (gap height)	• The filling time increases with the decrease of gap height. • Vacuum is more effective than gravity to promote the underfill flow.	[13]
1997	• Experiment (industrial standard) • FEM simulation with Hele-Shaw model • Analytical (Washburn equation)	• Flow visualization • Filling time measurement	• Viscosity, surface tension, and dynamic contact angle affected the filling time. • Washburn model with the incorporation of dynamic contact angle gave better filling time predictions than the static contact angle.	[18]
1999	• Experiment (industrial standard) • Plastic integrated circuit encapsulation-computer aided design simulation	• Flow visualization • Filling time measurement/ prediction	• The racing effect was observed for the first time where the edge flow is faster than the center flow.	[24]
1999	• Analytical (momentum equation)	• Filling time prediction	• The capillary flow of dense suspension mixture in plane channel was modeled to simulate the underfill process.	[65]

(continued)

Year	Research method	Research goal	Highlight on main finding	Reference
		• Analysis on the distribution of filler particles	• The redistribution of filler particle was presented, in which the particles travel from the walls toward the centerline as the flow progress.	
2002	• Analytical (Darcy's law)	• Flow visualization	• Capillary force parameter, F, increases with the gap height and bump diameter, indicating faster underfill flow.	[49,50]
	• FEM simulation of modified Hele-Shaw model with porous media assumption	• Filling time prediction	• There is a criticality of bump pitch in which F is maximal, and F remains constant with the further increase of pitch.	
		• Design optimization (bump pitch, bump diameter, and gap height)	• The flow resistances induced by chip, substrate, and bump were simulated and showed the edge effects during underfill flow.	
2002	• Experiment (industrial standard)	• Material characterization of underfill fluids	• The material properties and rheological behaviors of underfill fluids, i.e., surface tension, viscosity, and contact angle, were measured experimentally.	[36]
		• Design optimization (surface tension, viscosity, and contact angle)	• The surface energy of substrate needs to be higher than the surface tension of underfill fluid for better filling performance.	
2003	• Analytical formulation (Darcy's law)	• Flow visualization	• The contact line jump phenomenon was first theorized.	[51]
	• FEM simulation of modified Hele-Shaw model with porous media assumption	• Filling time prediction/ measurement	• The capillary action in underfilling flow was found to be anisotropic such that it varies with the filling direction and also caused the edge preferential flow observed in experiment.	
	• Experiment (glass plates of photoresists)			
2004	• Analytical formulation (regional segregation approach and momentum equation)	• Filling time prediction	• The regional segregation approach was introduced by computing the filling times separately at regions with and without bumps.	[74]
		• Design optimization (bump diameter, gap height, solder bump arrangement, and contact angle)	• The square root of filling time is approximately proportional to the filling distance.	
			• Smaller gap height and higher contact angle yield longer filling time, while the driving capillary pressure decreases with the bump density.	
2005	• Imitated experiment with glass slide	• Filling time measurement/ predi ction	• The glass slide flow test can reproduce the underfill flow, and the measured flow time is consistent to the prediction by Washburn equation.	[84]
	• Analytical (Washburn equation)	• Flow visualization	• The viscosity has the largest impact on the filling time, compared to the contact angle and surface tension.	
		• Design optimization (gap height)	• The increases of gap height decrease the flow time but increase the void formation occurrence.	
		• Package's reliability on voiding		
2005	• Analytical (momentum equation)	• Filling time prediction	• An analytical filling time model was developed based on the virtual work principle of averaged bump resistance pressure for non-Newtonian underfill fluid.	[22]
2005	• Analytical (momentum equation with transient term)	• Filling time prediction	• The influence of transient term on filling time is negligible when the viscosity is high (>0.1 Pa·s) and the gap height (~50 μm) is small, so the underfill flow is assumed to be steady.	[87]
			• Solder bump resistant possess significant effect on the underfill flow.	
2006	• Analytical (Darcy's law)	• Filling time prediction	• Small contact angle yields faster underfill flows.	[52]
	• FEM simulation with Hele-Shaw model	• Design optimization (bump pitch, bump arrangement, and contact angle)	• If the bump pitch is less than the critical value, the filling rate slowed down drastically. This critical pitch is dependent on gap height and bump diameter.	
			• Hexagonal bump arrangement has higher filling rate than the quadrilateral arrangement.	
2007	• Analytical formulation (momentum equation with rotational inertia term)	• Filling time prediction	• A new variation of flip-chip underfill process that is attached on the top of a rotating disk was proposed to enhance the capillary underfill flow and thus decrease the filling time.	[15]
2007	• Experiment (industrial standard)	• Material characterization of underfill fluids	• Underfill fluids with low and high filler loadings exhibit as Newtonian fluid and non-Newtonian fluid, respectively.	[35]
		• Flow visualization	• Underfill with small filler size exhibits yield stress and with fast flow time can reduce filler settling.	
		• Filling time measurement	• The void count can be reduced by decreasing the surface energy of substrate or increasing the viscosity.	
		• Package's reliability on voiding and filler settling		
2007	• Analytical formulation (momentum equation)	• Design optimization (bump pitch)	• There exists a critical clearance between bumps, in which the filling time lengthens significantly if the bump pitch is less than this critical value.	[80]

(continued)

Year	Research method	Research goal	Highlight on main finding	Reference
			• A design criterion of flip-chip package was devised according to the critical clearance (bump pitch).	
2008	• FDM numerical simulation	• Flow visualization	• New numerical simulation approach was introduced to simulate both capillary and no-flow underfill process.	[72]
2008	• Experiment (parallel plates of die and substrate, industrial standard package)	• Flow visualization Filling time measurement	• Washburn equation did not consider both the solder bump resistance and non-Newtonian behavior of underfill fluid, causing mismatch with the present experimental findings.	[26]
2009	FEM simulation with volume of fluid (ANSYS)	• Flow visualization • Filling time prediction	• ANSYS software was introduced to simulate the two-dimensional flow of non-Newtonian underfill fluid using the power-law.	[53]
2010	FVM simulation (ANSYS FLUENT)	• Flow visualization • Filling time prediction • Design optimization (bump arrangement)	Full array solder bump has the highest filling time, while the perimeter array has the shortest filling time.	[54]
2010	• Analytical (momentum equation)	• Filling time prediction	• The filling time was obtained analytically by solving the momentum equation with the fluid's viscosity modeled by the power-law.	[75]
2010	Experiment	Flow visualization	• Small bump pitch lengthens the filling time and has slower filling rate.	[81]
	• FEM simulation	• Filling time prediction/ measurement • Design optimization (bump pitch)	• Low bump density in the middle region of package and the adoption of flow channels can improve the uniformity of flow front and increase the filling time.	
2010, 2011	• Microparticle image velocimetry experiment	• Flow visualization	• The detailed meniscus behaviors of underfill flow advancement in bump array were studied while observing the contact line jump for the first time.	[27,28]
		• Filling time measurement	• The meniscus flow velocity was in-phase with the dynamic contact angle.	
		• Design optimization (bump pitch)	• The filling time over a fixed distance decreases with the increase in the bump pitch.	
2011	• Analytical (Darcy's law and porous media approach) • FEM simulation with control volume	• Flow visualization • Filling time prediction • Determination of underfill parameter—permeability of flip-chip domain • Design optimization (bump pitch and gap height)	• The viscosity and velocity profiles of non-Newtonian underfill fluid across the gap were studied at different pitches and heights. • The filling time increases with the power-law index of non-Newtonian fluid.	[78,79]
2011	• FVM simulation (ANSYS FLUENT) • Experiment	• Flow visualization • Filling time prediction • Design optimization (bump pitch)	• The decrease in pitch size slowed the underfill flow. • No edge effect was observed in the bump-free regions.	[19]
2012	• FVM simulation (ANSYS FLUENT)	• Flow visualization • Filling time prediction • Design optimization (gap height)	• Decreases in gap height increase the filling time, and this applied for both Newtonian and non-Newtonian underfill fluids.	[55,56]
2013	• FEM simulation • Analytical (Darcy's law)	• Filling time prediction • Determination of underfill parameter—permeability of flip-chip domain	• The permeability of flip-chip can be increased by increasing the bump pitch and bump height or decreasing the bump diameter and power-law index.	[82]
2014	• Analytical (Darcy's law) • FEM simulation	• Filling time prediction	• A new analytical filling time model was proposed by averaging the capillary pressure based on the mass conservation and also incorporating entrant and exit contact line jumps, which the flip-chip's permeability was computed numerically.	[21,76]
2016	• Analytical (Darcy's law)	• Filling time prediction	• An analytical filling time model was introduced with new formulations on the averaging of driving pressure and effective permeability.	[77]
2016	• FVM simulation	• Flow visualization	U-type dispensing gives the fastest underfill flow, followed by L-type and finally I-type	[30]
	• Scaled-up imitated experiment	• Filling time measurement • Design optimization (bump arrangement and dispensing type)	• Perimeter bump array registered shortest filling time, followed by middle empty and finally full array	
2016	• LBM simulation	• Flow visualization	• LBM numerical approach based with the generalized interparticle-potential model was developed to the model the capillary flow of underfill fluid in flip-chip package, which performed better than continuum surface force model in representing the capillary force for the simulation.	[17]

(continued)

Year	Research method	Research goal	Highlight on main finding	Reference
2016	• LBM simulation • FVM simulation	• Flow visualization • Filling time prediction • Design optimization (bump arrangement) • Package's reliability on voiding	• LBM simulation can predict voiding formation. • The middle empty bump arrangement most prone to void formation. • Voiding can be reduced using underfill fluid of higher Bond number and higher viscosity.	[45]
2016	• LBM simulation • FVM simulation • Scaled-up imitated experiment	• Flow visualization • Filling time prediction/ measure ment • Design optimization (bump arrangement) Package's reliability on voiding	• The increase in bump count reduces the pressure and flow velocity of underfill fluid. • LBM can simulate the void formation at higher precision than FVM.	[46]
2016	• FVM simulation with FSI using ANSYS System Coupling • Scaled-up imitated experiment	• Flow visualization • Filling time measurement	• In the newly introduced thermocapillary assisted underfill of multistacks BGA, the implementation of thermal gradient along the package layer can promote the underfill flow and reduce the filling time.	[16]
2017	• FVM simulation with discrete phase model	• Flow visualization • Filling time measurement • Analysis on the distribution of filler particles • Design optimization (filler contents)	• The underfill fluid was modeled as a colloid suspension of epoxy and nanosilica fillers using discrete phase model. • The higher the filler content, the slower the underfill flow, while the particles' accretion and erosion rates increase.	[5]
2017	• FVM simulation with FSI using ANSYS System Coupling • Scaled-up imitated experiment	• Flow visualization • Filling time measurement/ prediction • Design optimization (scale-size/gap height, bump arrangement, and dispensing type)	• BGA of larger scale size gives higher filling time at specific filling percentage. • The combination of U-type dispensing method and middle empty array gives the shortest filling time. • The velocity distribution of underfill fluid invariant with scaling, but the entrant pressure decreases upon being scaled-up.	[47,70,85]
2018	• FEM simulation (COMSOL MULTIPHYSICS)	• Flow visualization	• Dynamic pressure boundary condition method with surface force model was proposed to simulate the racing effect. • The racing effect can be alleviated by decreasing the dispensing length.	[62]
2018	• PIV experiment on scaled imitated package • FVM simulation • Analytical	• Flow visualization • Filling time prediction/ measurement • Design optimization (bump shape)	• Washburn equation has been modified to model the capillary underfill flow with triple inlet dispensing (U-shape). • Small neck diameter, low sphericity, and high pad-to-neck ratio are key factors for fast underfill flow; thus, concave-shape bump gives the lowest filling time.	[39]
2018	• Scaled-up imitated experiment • LBM simulation	• Flow visualization • Design optimization (gap height, bump arrangement, and dispensing types) Package's reliability on voiding	• U-type dispensing is more likely to cause void formation than L-type dispensing. • Smaller void was formed in the middle empty array compared to the full array. The size of void formed increases with the gap height.	[48]
2018	• Analytical (porous media permeability)	• Determination of underfill parameter—permeability of flip-chip domain	• The analytical models for pore permeability and superficial permeability of underfill flip-chip flow domain were derived. • An analytical permeability with the consideration of actual specific surface and tortuosity was formulated and comparable to the numerical permeability.	[88,89]
2019	• LBM simulation • Scaled-up imitated experiment	• Flow visualization • Filling time prediction/ measurement Package's reliability on voiding	• Pressurized underfill results in much shorter filling time than capillary underfill. • The flow pressure near the inlet region is up to four times of the inlet pressure, due to the reverse flow.	[12]
2019	• Analytical (regional segregation approach, and momentum equation)	• Filling time prediction	• A new analytical filling time model based on regional segregation approach for non-Newtonian fluid was developed by separating computing the filling times at bump, exit CLJ, and bumpless regions.	[23]
2019	• Analytical (regional segregation approach, and momentum equation)	• Design optimization (gap height, bump pitch, and contact angle)	• A filling time chart was developed, which gives the filling time at the different combinations of bump pitch, gap height, and contact angle.	[31]

(continued)

Year	Research method	Research goal	Highlight on main finding	Reference
	• Experiment (industrial standard)	• Filling time prediction	• There is a critical value of bump pitch which yields the lowest filling time. • The critical contact angle defined the variation trend of filling time with bump pitch.	
2019	• FVM simulation	• Flow visualization	• Shorter bump pitch gives slower underfill flow but faster filling completion.	[57]
		• Filling time prediction	• The formation and propagation of voids in package were simulated.	
		• Design optimization (bump shape) • Package's reliability on voiding	• The contact angle of underfill flow varies sinusoidally with time.	
2020	• LBM simulation	• Flow visualization	• The adhesive force between fluid and solid was affected by the density ratio of the fluids, while wall adhesive is affected by solder bump.	[66]
	• FVM simulation • Scaled-up imitated experiment		• LBM simulation gives better adhesive force prediction than FVM.	
2020	• LBM simulation	• Flow visualization	• Hourglass-shaped bump gives shorter filling time upon compared to the truncated sphere bump.	[67]
	• Scaled-up imitated experiment	• Filling time prediction/ measurement • Design optimization (bump shape)	• Further refinement on the curve profile of hourglass-shaped bump can reduce the filling time.	
2020	• FVM simulation	• Flow visualization	• Filling efficiency was introduced to quantify the productivity of underfill process.	[20]
	• Analytical (regional segregation approach, and momentum equation) • Scaled-up imitated experiment	• Filling time prediction/ measurement • Design optimization (bump pitch)	• The scaling of test vehicle for modeling the capillary underfill process is viable and yields similar flow behaviors, provided that the scaling factor is less than the scaling limit.	
2020	• Optimization statistical approaches (Taguchi method, gray relational analysis, and technique for order of preference by similarity to ideal solution) • Experiment	• Design optimization (preheat temperature, dispensing type, dispensing volume, and interval state)	• All four process operating parameters were optimized to attain the best underfill quality in terms of solder ball count, spread distance of residual underfill, and completion time.	[90]
2020	• FVM simulation	• Flow visualization	• The meniscus evolution and contact line jump were numerically simulated using micromesh unit-cell technique and analytically visualized for underfill flow in flip-chips of different bump pitches.	[71]
	• Analytical	• Package's reliability on voiding • Design optimization (bump pitch)	• A voiding mechanism was generated based on the spatial characteristic of underfill meniscus and its interaction on the bump during entrance contact line jump.	

Appendix B: Summary of Past Research Works on the Study of Underfilling Flow Stage in the Mold Encapsulation Process

Year	Research method	Research goal	Highlight on main finding	Reference
1998	• FEM simulation with Hele-Shaw model	• Flow visualization	• Molding pressure was affected by compression speed and stroke.	[91]
		• Filling time measurement/ prediction	• At fast injection melt speed, the compression mold reduces the molding pressure more than the injection mold.	
2000	• Experiment (industrial standard)	• Flow visualization	• The mold transfer process of TQFP was simulated and studied experimentally.	[25]
	• Plastic integrated circuit encapsulation-computer aided design simulation	• Filling time measurement/ prediction	• The resin conversion time is insufficient at the normal and high fill rates.	
2010	• FVM simulation (ANSYS FLUENT)	• Flow visualization	• The viscosity of the encapsulant decreases with temperature, while the shear rate increases with temperature.	[37]
	• Experiment (industrial standard)	• Filling time prediction/ measurement • Design optimization (temperature)	• The optimum temperature range of molding process is 200–260 °C.	
2010	• FVM simulation (ANSYS FLUENT)	• Flow visualization	• The number of void count increases with the number of vertical stacked dies and the row of stacked dies.	[38]

(continued)

Year	Research method	Research goal	Highlight on main finding	Reference
	• Experiment	• Filling time prediction/ measurement • Package's reliability on voiding		
2011	• Fluid–structure interaction • FSI simulation with FVM (ANSYS FLUENT) and FEM (ABAQUS) • Experiment	• Flow visualization • Filling time prediction/ measurement • Design optimization (inlet pressure) • Package's reliability on deformation	• The stress and strain on die increase with the inlet pressure. • Incomplete filling was observed near the corner and outlet region, while the percentage of voiding increases with the inlet pressure.	[59]
2011	• FVM simulation (ANSYS FLUENT)	• Flow visualization • Filling time prediction/ measurement • Package's reliability on voiding	• The usage of multigate inlet in TQFP mold encapsulation can reduce the filling time and the voids occurrence.	[58]
2012	• FSI simulation with FVM (ANSYS FLUENT) and FEM (ABAQUS) • Scaled-up imitated experiment	• Flow visualization • Filling time prediction/ measurement • Package's reliability on deformation and voiding	• The edge and middle regions of chip were deformed by the flow. • The flow mechanism of molding process was presented to visualize the air trap phenomenon.	[29]
2012	• FVM numerical simulation • Scaled-up imitated experiment	• Flow visualization • Filling time prediction/ measure ment • Package's reliability on voiding	• Unstable flow front can cause void formation. • The chips' stacking further increases the voiding. • Typical inlet gate causes less voids than diagonal and top center inlet gates.	[40]
2012	• Statistical response surface methodology • FSI simulation with FVM (ANSYS FLUENT) and FEM (ABAQUS)	• Design optimization (bump height, chip thickness, mold gapwise, and inlet pressure) • Package's reliability on deformation and voiding	• All parameters were optimized to minimize the package's stress and deformation as well as the void formation. • Filling time was mainly affected only by the inlet pressure.	[92]
2012	• FSI simulation with FVM (ANSYS FLUENT) and FEM (ABAQUS)	• Flow visualization • Filling time prediction/ measurement • Package's reliability on deformation and voiding • Design optimization (bump shape and input/output count)	• Increased in input/output count can reduce the displacement and stress on the chip structure. • Cylindrical bump shape yields the lowest stress on bump and chip as well as minimizes the void formation.	[42]
2012	• FSI simulation with FVM (ANSYS FLUENT) and FEM (ABAQUS) • Scaled-up imitated experiment	• Flow visualization • Filling time prediction/ measurement • Package's reliability on deformation	• For the plastics ball grid array packages with stacked dies, the increase in inlet pressure increased the wire sweep, and the wires deformed easily due to the increase in wire span.	[61]
2012	• FSI simulation with FVM (ANSYS FLUENT) and FEM (ABAQUS) • Scaled-up imitated experiment	• Flow visualization • Filling time prediction/ measurement • Package's reliability on deformation and voiding	• The middle region of chip without the bump support deformed downward with the highest displacement, while the edge of chip bends upward. • Stacked-chip package has more void formation.	[41]
2013	• FVM simulation (ANSYS FLUENT)	• Flow visualization • Filling time prediction • Package's reliability on voiding • Design optimization (bump pitch)	• Smaller bump pitch causes slower filling rate, higher pressure distribution, larger conversion rate, and more voids' formation.	[93]
2014	• FSI simulation with FVM (ANSYS FLUENT) and FEM (ABAQUS) • Scaled-up imitated experiment	• Flow visualization • Filling time prediction/ measurement • Package's reliability on deformation	• Both the displacement and stress of stacked-chip structure increase with the number of stacking layers.	[44]

(continued)

Year	Research method	Research goal	Highlight on main finding	Reference
		• Design optimization (chip stacking layer)		
2014	• FSI simulation with FVM (ANSYS FLUENT) and FEM (ABAQUS) • Scaled-up imitated experiment	• Flow visualization • Filling time prediction/ measurement • Package's reliability on deformation and voiding • Design optimization (bump arrangement)	• Deformation was generally observed on the bumpless region close to the inlet gate. • The highest deformation and stress were found on the structure of the package with perimeter bump array.	[43]
2015	• FEM simulation • Transparent imitated experiment	• Flow visualization • Package's reliability on voiding • Design optimization (vacuum quality, aspect ratio, arrangement, and thickness)	• Better vacuum quality (i.e., closer to 0 Pa) yields voids of smaller size. • Aspect ratio, arrangement, and chip thickness affected the mold underfill flow. • The addition of solid glue sticks in the gap of chip array can reduce voiding.	[14,94]
2016	• LBM simulation	• Flow visualization • Filling time prediction • Design optimization (stacking layout) • Package's reliability on voiding	• The formation of microvoid ($<$100 μm) in the stacked chips was simulated using LBM. • Stacking layout affected the microvoids formed in the region of stacked chips.	[68]
2017	• FVM simulation with FSI using ANSYS System Coupling • Scaled-up imitated experiment	• Flow visualization • Filling time measurement/ predi ction • Package's reliability on deformation and voiding • Design optimization (aspect ratio and stacking layout)	• The deformation and stress of chip, as well as the void percentage, increase with its aspect ratio. • The optimum aspect ratio is 2. • The stacking layout of stacked chips influenced the flow and structural aspects. • The maximal stress occurred at the middle region of the top chip.	[63,95]
2019	• Statistical response surface methodology • FVM simulation with FSI using ANSYS System Coupling	• Design optimization (bump height, chip thickness, aspect ratio, and inlet pressure) • Package's reliability on deformation and voiding	• All parameters of bump height, chip thickness, aspect ratio, and inlet pressure were optimized for the mold underfill process to minimize the package's deformation and voiding.	[69]

Appendix C: Summary of Past Research Works on the Study of Underfilling Flow Stage That Involved Alternative Encapsulation Process, Other Than the Capillary and Mold Underfill Processes

Year	Type of underfill process	Research method	Research goal	Highlight on main finding	Reference
1996	• Capillary • Gravity assisted • Vacuum-assisted	• Analytical (Washburn equation) • Experiment (parallel plate)	• Filling time measurement/ prediction • Design optimization (gap height)	• The filling time increases with the decrease of gap height • Vacuum is more effective than gravity to promote the underfill flow.	[13]
1997	• Pressurized	• Experiment (industrial standard) • FEM simulation with Hele-Shaw model	• Filling time measurement	• The pressurized underfill is about 1000 times faster than the capillary underfill. • The package cavity can be filled completely with pressurized underfill, so the package's reliability can be increased.	[10]
1998	• No-flow	• FEM simulation (POLYFLOW)	• Flow visualization • Package's reliability on voiding • Design optimization (bump pitch and bump diameter) and operating temperature	• Both placement force and void occurrence can be decreased with the increase in bump pitch and size. • Increased in the temperature can reduce the placement force but causes extensive void formation.	[83]
2007	• Rotational-assisted	• Analytical formulation (momentum equation with	• Filling time prediction	• A new variation of flip-chip underfill process that is attached on the top of a rotating	[15]

(continued)

Year	Type of underfill process	Research method	Research goal	Highlight on main finding	Reference
	• Capillary	rotational inertia term)		disk was proposed to enhance the capillary underfill flow and thus decrease the filling time.	
2008	• Capillary • No-flow	• FDM numerical simulation	• Flow visualization	• New numerical simulation approach was introduced to simulate both capillary and no-flow underfill process.	[72]
2010	• Pressurized	• FVM simulation (ANSYS FLUENT)	• Flow visualization • Filling time prediction • Design optimization (dispensing type)	• U-type dispensing gives shortest filling time but is prone to void formation; thus, L-type dispensing is optimum on the balance of filling time and voiding.	[11]
2016	• Thermocapillary	• FVM simulation with FSI using ANSYS System Coupling • Scaled-up imitated experiment	• Flow visualization • Filling time measurement	• In the newly introduced thermocapillary assisted underfill of multistacks BGA, the implementation of thermal gradient along the package layer can promote the underfill flow and reduce the filling time.	[16]
2019	• Capillary • Pressurized	• LBM simulation • Scaled-up imitated experiment	• Flow visualization • Filling time prediction/measurement • Package's reliability on voiding	• Pressurized underfill results in much shorter filling time than capillary underfill. • The flow pressure near the inlet region is up to four times of the inlet pressure, due to the reverse flow.	[12]
2020	• No-flow	• FVM simulation • Scaled-up imitated experiment	• Flow visualization • Filling time prediction/measurement • Design optimization (no-flow dispensing pattern) • Package's reliability on voiding	• The no-flow filling times for all dispensing methods are almost similar. • Combined (dot and cross) pattern yields the best filling completion but prone to void formation. • Dot pattern has the least void formation as it gives high pressure underfill flows.	[60]

References

[1] Wong, C. P., Luo, S., and Zhang, Z., 2000, "Flip the Chip," Science, **290**(5500), pp. 2269–2270.
[2] Wan, J. W., Zhang, W. J., and Bergstrom, D. J., 2007, "Recent Advances in Modeling the Underfill Process in Flip-Chip Packaging," Microelectron. J., **38**(1), pp. 67–75.
[3] Zhang, Z., and Wong, C. P., 2004, "Recent Advances in Flip-Chip Underfill: Materials, Process, and Reliability," IEEE Trans. Adv. Packag., **27**(3), pp. 515–524.
[4] Fang, K., 2019, "3—Encapsulation Process Technology," *Encapsulation Technologies for Electronic Applications*, 2nd ed. (Materials and Processes for Electronic Applications), H. Ardebili, J. Zhang, and M. G. Pecht, eds., William Andrew Publishing, Cambridge, MA, pp. 123–181.
[5] Ng, F. C., Abas, A., Gan, Z. L., Abdullah, M. Z., Che Ani, F., and Yusuf Tura Ali, M., 2017, "Discrete Phase Method Study of Ball Grid Array Underfill Process Using Nano-Silica Filler-Reinforced Composite-Encapsulant With Varying Filler Loadings," Microelectron. Reliab., **72**, pp. 45–64.
[6] Kim, Y. B., and Sung, J., 2012, "Capillary-Driven Micro Flows for the Underfill Process in Microelectronics Packaging," J. Mech. Sci. Technol., **26**(12), pp. 3751–3759.
[7] Khor, C. Y., Abdullah, M. Z., Lau, C. S., and Azid, I. A., 2014, "Recent Fluid-Structure Interaction Modeling Challenges in IC encapsulation—A Review," Microelectron. Reliab., **54**(8), pp. 1511–1526.
[8] Lee, S., Yim, M. J., Master, R. N., Wong, C. P., and Baldwin, D. F., 2008, "Void Formation Study of Flip Chip in Package Using No-Flow Underfill," IEEE Trans. Electron. Packag. Manuf., **31**(4), pp. 297–305.
[9] Lee, S., Yim, M. J., and Baldwin, D., 2009, "Void Formation Mechanism of Flip Chip in Package Using No-Flow Underfill," ASME J. Electron. Packag., **131**(3), p. 031014.
[10] Han, S., and Wang, K. K., 1997, "Study on the Pressurized Underfill Encapsulation of Flip Chips," IEEE Trans. Compon., Packag., Manuf. Technol., Part B, **20**(4), pp. 434–442.
[11] Khor, C. Y., Abdul Mujeebu, M., Abdullah, M. Z., and Ani, F. C., 2010, "Finite Volume Based CFD Simulation of Pressurized Flip-Chip Underfill Encapsulation Process," Microelectron. Reliab., **50**(1), pp. 98–105.
[12] Gan, Z. L., Abas, A., Ishak, M. H. H., Abdullah, M. Z., and Ngang, J. L., 2019, "Comparative Study of Pressurized and Capillary Underfill Flow Using Lattice Boltzmann Method," Arabian J. Sci. Eng., **44**(9), pp. 7627–7652.
[13] Schwiebert, M. K., and Leong, W. H., 1996, "Underfill Flow as Viscous Flow Between Parallel Plates Driven by Capillary Action," IEEE Trans. Compon., Packag., Manuf. Technol., Part C, **19**(2), pp. 133–137.
[14] Guo, X. R., and Young, W. B., 2015, "Vacuum Effect on the Void Formation of the Molded Underfill Process in Flip Chip Packaging," Microelectron. Reliab., **55**(3–4), pp. 613–622.
[15] Lin, C. M., Chang, W. J., and Fang, T. H., 2007, "Flip-Chip Underfill Packaging Considering Capillary Force, Pressure Difference, and Inertia Effects," ASME J. Electron. Packag., **129**(1), pp. 48–55.
[16] Ng, F. C., Abas, A., Ishak, M. H. H., Abdullah, M. Z., and Aziz, A., 2016, "Effect of Thermocapillary Action in the Underfill Encapsulation of Multi-Stack Ball Grid Array," Microelectron. Reliab., **66**, pp. 143–160.
[17] Wang, H., Hao, X., Zhou, H., Zhang, Y., and Li, D., 2016, "Underfill Flow Simulation Based on Lattice Boltzmann Method," Microelectron. Eng., **149**, pp. 66–72.
[18] Han, S., and Wang, K. K., 1997, "Analysis of the Flow of Encapsulant During Underfill Encapsulation of Flip-Chips," IEEE Trans. Compon., Packag., Manuf. Technol., Part B, **20**(4), pp. 424–433.
[19] Lee, S. H., Lee, H. J., Kim, J. M., and Shin, Y. E., 2011, "Dynamic Filling Characteristics of a Capillary Driven Underfill Process in Flip-Chip Packaging," Mater. Trans., **52**(10), pp. 1998–2003.
[20] Ng, F. C., Abas, M. A., and Abdullah, M. Z., 2019, "Filling Efficiency of Flip-Chip Underfill Encapsulation Process," Soldering Surf. Mount Technol., **32**(1), pp. 10–18.
[21] Yao, X. J., Wang, Z. D., and Zhang, W. J., 2014, "A New Analysis of the Capillary Driving Pressure for Underfill Flow in Flip-Chip Packaging," IEEE Trans. Compon., Packag., Manuf. Technol., **4**(9), pp. 1534–1544.
[22] Wan, J. W., Zhang, W. J., and Bergstrom, D. J., 2005, "An Analytical Model for Predicting the Underfill Flow Characteristics in Flip-Chip Encapsulation," IEEE Trans. Adv. Packag., **28**(3), pp. 481–487.
[23] Ng, F. C., Abas, A., and Abdullah, M. Z., 2019, "Regional Segregation With Spatial Considerations-Based Analytical Filling Time Model for Non-Newtonian Power-Law Underfill Fluid in Flip-Chip Encapsulation," ASME J. Electron. Packag., **141**(4), p. 041009.
[24] Nguyen, L., Quentin, C., Fine, P., Cobb, B., Bayyuk, S., Yang, H., and Bidstrup-Allen, S. A., 1999, "Underfill of Flip Chip on Laminates: Simulation and Validation," IEEE Trans. Compon. Packag. Technol., **22**(2), pp. 168–176.
[25] Nguyen, L., Quentin, C., Lee, W., Bayyuk, S., Bidstrup-Allen, S. A., and Wang, S.-T., 2000, "Computational Modeling and Validation of the Encapsulation of Plastic Packages by Transfer Molding," ASME J. Electron. Packag., **122**(2), pp. 138–146.
[26] Wan, J. W., Zhang, W. J., and Bergstrom, D. J., 2008, "Experimental Verification of Models for Underfill Flow Driven by Capillary Forces in Flip-Chip Packaging," Microelectron. Reliab., **48**(3), pp. 425–430.
[27] Lee, S. H., Sung, J., and Kim, S. E., 2010, "Dynamic Flow Measurements of Capillary Underfill Through a Bump Array in Flip Chip Package," Microelectron. Reliab., **50**(12), pp. 2078–2083.
[28] Kim, Y. B., Sung, J., and Lee, M. H., 2011, "Micro-PIV Measurements of Capillary Underfill Flows and Effect of Bump Pitch on Filling Process," J. Visualization, **14**(3), pp. 237–248.

[29] Khor, C. Y., Abdullah, M. Z., and Leong, W. C., 2012, "Visualization of Fluid/Structure Interaction in IC Encapsulation," IEEE Trans. Compon., Packag., Manuf. Technol., **2**(8), pp. 1239–1246.
[30] Abas, A., Haslinda, M. S., Ishak, M. H. H., Nurfatin, A. S., Abdullah, M. Z., and Che Ani, F., 2016, "Effect of ILU Dispensing Types for Different Solder Bump Arrangements on CUF Encapsulation Process," Microelectron. Eng., **163**, pp. 83–97.
[31] Ng, F. C., Ali, M. Y. T., Abas, A., Khor, C. Y., Samsudin, Z., and Abdullah, M. Z., 2019, "A Novel Analytical Filling Time Chart for Design Optimization of Flip-Chip Underfill Encapsulation Process," Int. J. Adv. Manuf. Technol., **105**(7–8), pp. 3521–3530.
[32] Sun, Y., Zhang, Z., and Wong, C. P., 2006, "Study and Characterization on the Nanocomposite Underfill for Flip Chip Applications," IEEE Trans. Compon. Packag. Technol., **29**(1), pp. 190–197.
[33] Sun, Y., Zhang, Z., and Wong, C. P., 2005, "Study on Mono-Dispersed Nano-Size Silica by Surface Modification for Underfill Applications," J. Colloid Interface Sci., **292**(2), pp. 436–444.
[34] Shan, X., and Chen, Y., 2018, "Experimental and Modeling Study on Viscosity of Encapsulant for Electronic Packaging," Microelectron. Reliab., **80**, pp. 42–46.
[35] Wang, J., 2007, "The Effects of Rheological and Wetting Properties on Underfill Filler Settling and Flow Voids in Flip Chip Packages," Microelectron. Reliab., **47**(12), pp. 1958–1966.
[36] Wang, J., 2002, "Underfill of Flip Chip on Organic Substrate: Viscosity, Surface Tension, and Contact Angle," Microelectron. Reliab., **42**(2), pp. 293–299.
[37] Khor, C. Y., Ariff, Z. M., Ani, F. C., Mujeebu, M. A., Abdullah, M. K., Abdullah, M. Z., and Joseph, M. A., 2010, "Three-Dimensional Numerical and Experimental Investigations on Polymer Rheology in Meso-Scale Injection Molding," Int. Commun. Heat Mass Transfer, **37**(2), pp. 131–139.
[38] Khor, C. Y., Abdullah, M. K., Abdullah, M. Z., Mujeebu, M. A., Ramdan, D., Majid, M. F. M. A., and Ariff, Z. M., 2010, "Effect of Vertical Stacking Dies on Flow Behavior of Epoxy Molding Compound During Encapsulation of Stacked-Chip Scale Packages," Heat Mass Transfer, **46**(11–12), pp. 1315–1325.
[39] Ng, F. C., Abas, A., and Abdullah, M. Z., 2018, "Effect of Solder Bump Shapes on Underfill Flow in Flip-Chip Encapsulation Using Analytical, Numerical and PIV Experimental Approaches," Microelectron. Reliab., **81**, pp. 41–63.
[40] Khor, C. Y., Abdullah, M. Z., Ariff, Z. M., and Leong, W. C., 2012, "Effect of Stacking Chips and Inlet Positions on Void Formation in the Encapsulation of 3D Stacked Flip-Chip Package," Int. Commun. Heat Mass Transfer, **39**(5), pp. 670–680.
[41] Khor, C. Y., and Abdullah, M. Z., 2012, "Modelling and Analysis of the Effect of Stacking Chips With TSVs in 3D IC Package Encapsulation Process," Maejo Int. J. Sci. Technol., **6**(2), pp. 159–185.
[42] Khor, C. Y., Abdullah, M. Z., and Leong, W. C., 2012, "Fluid/Structure Interaction Analysis of the Effects of Solder Bump Shapes and Input/Output Counts on Moulded Packaging," IEEE Trans. Compon., Packag., Manuf. Technol., **2**(4), pp. 604–616.
[43] Khor, C. Y., Abdullah, M. Z., Lau, C. S., Leong, W. C., and Abdul Aziz, M. S., 2014, "Influence of Solder Bump Arrangements on Molded IC Encapsulation," Microelectron. Reliab., **54**(4), pp. 796–807.
[44] Ong, E. E. S., Abdullah, M. Z., Khor, C. Y., Loh, W. K., Ooi, C. K., and Chan, R., 2014, "Fluid-Structure Interaction Analysis on the Effect of Chip Stacking in a 3D Integrated Circuit Package With Through-Silicon Vias During Plastic Encapsulation," Microelectron. Eng., **113**, pp. 40–49.
[45] Abas, A., Gan, Z. L., Ishak, M. H. H., Abdullah, M. Z., and Khor, S. F., 2016, "Lattice Boltzmann Method of Different BGA Orientations on I-Type Dispensing Method," PLoS One, **11**(7), p. e0159357.
[46] Abas, A., Ishak, M. H. H., Abdullah, M. Z., Ani, F. C., and Khor, S. F., 2016, "Lattice Boltzmann Method Study of BGA Bump Arrangements on Void Formation," Microelectron. Reliab., **56**, pp. 170–181.
[47] Ng, F. C., Abas, M. A., Abdullah, M. Z., Ishak, M. H. H., and Chong, G. Y., 2017, "CUF Scaling Effect on Contact Angle and Threshold Pressure," Soldering Surf. Mount Technol., **29**(4), pp. 173–190.
[48] Abas, A., Ng, F. C., Gan, Z. L., Ishak, M. H. H., Abdullah, M. Z., and Chong, G. Y., 2018, "Effect of Scale Size, Orientation Type and Dispensing Method on Void Formation in the CUF Encapsulation of BGA," Sadhana - Acad. Proc. Eng. Sci., **43**(4), p. 0059.
[49] Young, W. B., and Yang, W. L., 2002, "The Effect of Solder Bump Pitch on the Underfill Flow," IEEE Trans. Adv. Packag., **25**(4), pp. 537–542.
[50] Young, W. B., and Yang, W. L., 2002, "Underfill Viscous Flow Between Parallel Plates and Solder Bumps," IEEE Trans. Compon. Packag. Technol., **25**(4), pp. 695–700.
[51] Young, W. B., 2003, "Anisotropic Behavior of the Capillary Action in Flip Chip Underfill," Microelectron. J., **34**(11), pp. 1031–1036.
[52] Young, W. B., and Yang, W. L., 2006, "Underfill of Flip-Chip: The Effect of Contact Angle and Solder Bump Arrangement," IEEE Trans. Adv. Packag., **29**(3), pp. 647–653.
[53] Wan, J. W., Zhang, W. J., and Bergstrom, D. J., 2009, "Numerical Modeling for the Underfill Flow in Flip-Chip Packaging," IEEE Trans. Compon. Packag. Technol., **32**(2), pp. 227–234.
[54] Khor, C. Y., Abdullah, M. Z., Abdul Mujeebu, M., and Ani, F. C., 2010, "FVM Based Numerical Study on the Effect of Solder Bump Arrangement on Capillary Driven Flip Chip Underfill Process," Int. Commun. Heat Mass Transfer, **37**(3), pp. 281–286.
[55] Khor, C. Y., Abdullah, M. Z., and Mujeebu, M. A., 2012, "Influence of Gap Height in Flip Chip Underfill Process With Non-Newtonian Flow Between Two Parallel Plates," ASME J. Electron. Packag., **134**(1), p. 011003.
[56] Khor, C. Y., Abdullah, M. Z., and Ani, F. C., 2012, "Underfill Process for Two Parallel Plates and Flip Chip Packaging," Int. Commun. Heat Mass Transfer, **39**(8), pp. 1205–1212.
[57] Ng, F. C., Abas, A., and Abdullah, M. Z., 2019, "Finite Volume Method Study on Contact Line Jump Phenomena and Dynamic Contact Angle of Underfill Flow in Flip-Chip of Various Bump Pitches," IOP Conf. Ser.: Mater. Sci. Eng., **530**(1), p. 012012.
[58] Khor, C. Y., Abdullah, M. Z., Abdullah, M. K., Mujeebu, M. A., Ramdan, D., Majid, M. F. M. A., Ariff, Z. M., and Rahman, M. A., 2011, "Numerical Analysis on the Effects of Different Inlet Gates and Gap Heights in TQFP Encapsulation Process," Int. J. Heat Mass Transfer, **54**(9–10), pp. 1861–1870.
[59] Khor, C. Y., Abdullah, M. Z., and Ani, F. C., 2011, "Study on the Fluid/Structure Interaction at Different Inlet Pressures in Molded Packaging," Microelectron. Eng., **88**(10), pp. 3182–3194.
[60] Nashrudin, M. N., Abas, M. A., Abdullah, M. Z., Ali, M. Y. T., and Samsudin, Z., 2021, "Study of Different Dispensing Patterns of No-Flow Underfill Using Numerical and Experimental Methods," ASME J. Electron. Packag., **143**(3), p. 031005.
[61] Ramdan, D., Abdullah, M. Z., Khor, C. Y., Leong, W. C., Loh, W. K., Ooi, C. K., and Ooi, R. C., 2012, "Fluid/Structure Interaction Investigation in PBGA Packaging," IEEE Trans. Compon., Packag., Manuf. Technol., **2**(11), pp. 1786–1795.
[62] Zhu, W., Wang, K., and Wang, Y., 2018, "A Novel Model for Simulating the Racing Effect in Capillary-Driven Underfill Process in Flip Chip," J. Micromech. Microeng., **28**(4), p. 045002.
[63] Ishak, M. H. H., Abdullah, M. Z., Aziz, M. A., Saad, A. A., Abdullah, M. K., Loh, W. K., Ooi, R. C., and Ooi, C. K., 2017, "Study on the Fluid–Structure Interaction at Different Layout of Stacked Chip in Molded Packaging," Arabian J. Sci. Eng., **42**(11), pp. 4743–4757.
[64] Zhou, S., and Sun, Y., 2012, "Multiscale, Multiphysics Model of Underfill Flow for Flip-Chip Packages," IEEE Trans. Compon., Packag., Manuf. Technol., **2**(6), pp. 893–902.
[65] Guo, Y., Lehmann, G. L., Driscoll, T., and Cotts, E. J., 1999, "A Model of the Underfill Flow Process: Particle Distribution Effects," Electronic Components and Technology Conference, San Diego, CA, June 1–4, pp. 71–76.
[66] Ishak, M. H. H., Ismail, F., Abdul Aziz, M. S., and Abdullah, M. Z., 2020, "Effect of Adhesive Force on Underfill Process Based on Lattice Boltzmann Method," Microelectron. Int., **37**(1), pp. 54–63.
[67] Nashrudin, M. N., Gan, Z. L., Abas, A., Ishak, M. H. H., and Tura Ali, M. Y., 2020, "Effect of Hourglass Shape Solder Joints on Underfill Encapsulation Process: Numerical and Experimental Studies," Soldering Surf. Mount Technol., **32**(3), pp. 147–156.
[68] Ishak, M. H. H., Abdullah, M. Z., and Abas, A., 2016, "Lattice Boltzmann Method Study of Effect Three Dimensional Stacking-Chip Package Layout on Micro-Void Formation During Encapsulation Process," Microelectron. Reliab., **65**, pp. 205–216.
[69] Ishak, M. H. H., Ismail, F., Aziz, M. S. A., Abdullah, M. Z., and Abas, A., 2019, "Optimization of 3D IC Stacking Chip on Molded Encapsulation Process: A Response Surface Methodology Approach," Int. J. Adv. Manuf. Technol., **103**(1–4), pp. 1139–1153.
[70] Ng, F. C., Abas, A., Abdullah, M. Z., Ishak, M. H. H., and Chong, G. Y., 2017, "Comparative Study of the Scaling Effect on Pressure Profiles in Capillary Underfill Process," IOP Conf. Ser. Mater. Sci. Eng., **203**(1), p. 012012.
[71] Ng, F. C., Zawawi, M. H., and Abas, M. A., 2020, "Spatial Analysis of Underfill Flow in Flip-Chip Encapsulation," Soldering Surf. Mount Technol., **33**(2), pp. 112–127.
[72] Hashimoto, T., Shin-Ichiro, T., Morinishi, K., and Satofuka, N., 2008, "Numerical Simulation of Conventional Capillary Flow and No-Flow Underfill in Flip-Chip Packaging," Comput. Fluids, **37**(5), pp. 520–523.
[73] Wang, H., Zhou, H., Zhang, Y., Li, D., and Xu, K., 2011, "Three-Dimensional Simulation of Underfill Process in Flip-Chip Encapsulation," Comput. Fluids, **44**(1), pp. 187–201.
[74] Young, W. B., 2004, "Capillary Impregnation Into Cylinder Banks," J. Colloid Interface Sci., **273**(2), pp. 576–580.
[75] Young, W. B., 2010, "Modeling of a Non-Newtonian Flow Between Parallel Plates in a Flip Chip Encapsulation," Microelectron. Reliab., **50**(7), pp. 995–999.
[76] Yao, X. J., Wang, Z., Zhang, W., and Zhou, X., 2014, "A New Model for Permeability of Porous Medium in the Case of Flip-Chip Packaging," IEEE Trans. Compon., Packag., Manuf. Technol., **4**(8), pp. 1265–1275.
[77] Luo, W., Liang, J. J., Zhang, Y., and Zhou, H. M., 2016, "An Analytical Model for the Underfill Flow Driven by Capillary Forces in Chip Packaging," 17th International Conference on Electronic Packaging Technology (ICEPT), Wuhan, China, Aug. 16–19, pp. 1381–1386.
[78] Young, W. B., 2011, "Effect on Filling Time for a Non-Newtonian Flow During the Underfilling of a Flip Chip," IEEE Trans. Compon., Packag., Manuf. Technol., **1**(7), pp. 1048–1053.
[79] Young, W. B., 2011, "Non-Newtonian Flow Formulation of the Underfill Process in Flip-Chip Packaging," IEEE Trans. Compon., Packag., Manuf. Technol., **1**(12), pp. 2033–2037.
[80] Wan, J. W., Zhang, W. J., and Bergstrom, D. J., 2007, "A Theoretical Analysis of the Concept of Critical Clearance Toward a Design Methodology for the Flip-Chip Package," ASME J. Electron. Packag., **129**(4), pp. 473–478.
[81] Peng, S. W., and Young, W. B., 2010, "Application of the Underfill Model to Bump Arrangement and Dispensing Process Design," IEEE Trans. Electron. Packag. Manuf., **33**(2), pp. 122–128.
[82] Yang, C., and Young, W. B., 2013, "The Effective Permeability of the Underfill Flow Domain in Flip-Chip Packaging," Appl. Math. Modell., **37**(3), pp. 1177–1186.

[83] Pascarella, N. W., and Baldwin, D. F., 1998, "Compression Flow Modeling of Underfill Encapsulants for Low Cost Flip Chip Assembly," IEEE Trans. Compon., Packag., Manuf. Technol., Part C, **21**(4), pp. 325–335.
[84] Wang, J., 2005, "Flow Time Measurements for Underfills in Flip-Chip Packaging," IEEE Trans. Compon. Packag. Technol., **28**(2), pp. 366–370.
[85] Ng, F., Abas, C. A., Abdullah, M. Z., Ishak, M. H. H., and Chong, G. Y., 2017, "Scaling Effect on Velocity Profiles in Capillary Underfill Flow," IOP Conf. Ser. Mater. Sci. Eng., **203**(1), p. 012013.
[86] Zhang, W. J., and van Luttervelt, C. A., 2011, "Toward a Resilient Manufacturing System," CIRP Ann. - Manuf. Technol., **60**(1), pp. 469–472.
[87] Wan, J. W., Zhang, W. J., and Bergstrom, D. J., 2005, "Influence of Transient Flow and Solder Bump Resistance on Underfill Process," Microelectron. J., **36**(8), pp. 687–693.
[88] Yao, X. J., and Zhang, W. J., 2018, "An Analytical Model for Permeability of Underfill Flow in Flip-Chip Packaging With Consideration of the Actual Specific Surface and Tortuosity," IEEE Trans. Compon., Packag., Manuf. Technol., **8**(8), pp. 1507–1514.
[89] Yao, X. J., Fang, J. J., and Zhang, W., 2018, "A Further Study on the Analytical Model for the Permeability in Flip-Chip Packaging," ASME J. Electron. Packag., **140**(1), p. 011001.
[90] Huang, C. Y., Shen, L. C., Wu, T. H., and Greene, C., 2020, "Application of Multi-Quality Parameter Design in the Optimization of Underfilling Process—A Case Study of a Vehicle Electronic Module," Soldering Surf. Mount Technol., **33**(2), pp. 128–138.
[91] Chen, S. C., Chen, Y. C., Cheng, N. T., and Huang, M. S., 1998, "Simulation of Injection-Compression Mold-Filling Process," Int. Commun. Heat Mass Transfer, **25**(7), pp. 907–917.
[92] Khor, C. Y., and Abdullah, M. Z., 2012, "Optimization of IC Encapsulation Considering Fluid/Structure Interaction Using Response Surface Methodology," Simul. Modell. Pract. Theory, **29**, pp. 109–122.
[93] Ong, E. E., Abdullah, M. Z., Khor, C. Y., Leong, W. C., Loh, W. K., Ooi, C. K., and Chan, R., 2013, "Numerical Modeling and Analysis of Microbump Pitch Effect in 3D IC Package With TSV During Molded Underfill (MUF)," Eng. Appl. Comput. Fluid Mech., **7**(2), pp. 210–222.
[94] Guo, X. R., and Young, W. B., 2015, "A Two-Dimensional Simulation Model for the Molded Underfill Process in Flip Chip Packaging," J. Mech. Sci. Technol., **29**(7), pp. 2967–2974.
[95] Ishak, M. H. H., Abdullah, M. Z., Abdul Aziz, M. S., Abas, A., Loh, W. K., Ooi, R. C., and Ooi, C. K., 2017, "Effects of Aspect Ratio in Moulded Packaging Considering Fluid/Structure Interaction: A CFD Modelling Approach," J. Appl. Fluid Mech., **10**(6), pp. 1799–1811.